Journal of Computational and Applied Mechanics, Vol. 4., No. 2., (2003), pp. 97–104

LOCAL BOUNDARY CONDITIONS WITH A HIGH-RESOLUTION NUMERICAL SCHEME FOR NON-OSCILLATORY SHOCK ABSORPTION AND REFLECTION

Satya Baboolal
Department of Computer Science, University of Durban-Westville
Private Bag X54001, Durban 4000, South Africa
sbab@pixie.udw.ac.za

Richard Naidoo
Department of Mathematics and Physics, Durban Institute of Technology
P.O. Box 1334, Durban 4000, South Africa
naidoor@yoda.cs.udw.ac.za

[Received: July 24, 2002]

Abstract. In this work we examine some simple non-oscillatory boundary conditions that can be applied to a typical class of modern finite-difference shock capturing schemes. In particular we concentrate on a non-staggered source-term version of the Nessyahu-Tadmor scheme [3] applied to some one-dimensional model equations admitting shocks that can interact with the system boundaries.

Mathematical Subject Classification: 65M06, 35L65, 35L67
Keywords: boundary conditions, shock capturing, high resolution schemes

1. Introduction

Recently many schemes have been employed in numerical studies of hyperbolic systems. Such systems occur in a wide variety of problems, including shock propagation in fluids [1]. New methods for the numerical solution of such systems fall into several classes, of which the fully discrete schemes of Nessyahu and Tadmor [2] and their extensions constitute one important class of Riemann-solver-free schemes for shock propagation problems. Here we concentrate on a non-staggered variation [3] of [2] and pay particular attention to what transpires on a wave structure at a boundary, especially when it is to be fully absorbed and when it is to be reflected. To illustrate the application of these two types of boundary conditions, we examine their effect on shock structures modelled by such equations as the inviscid Burgers' equation and the equations for a Broadwell gas, which is a two-dimensional neutral gas model allowing

for one-dimensional spatial variation. We formulate and test local boundary conditions required to smoothly absorb and to smoothly reflect shocks at the boundaries. Because of the spatial extent of the finite-difference grid stencils of modern high resolution schemes, it is required to employ "thick" boundary conditions, whereby, not only a single end point is treated as a boundary point but so too are its immediate neighbours. Tests conducted with this device in conjunction with the above [3] high resolution scheme indicate that simple local conditions can indeed result in smooth boundary interactions.

2. **Model equations and the numerical scheme**

The model equations studied are of the type,

$$\frac{\partial u(x,t)}{\partial t} + \frac{\partial f\,(u)}{\partial x} = g\,(u)\,, \tag{2.1}$$

a one-dimensional hyperbolic system [1] of partial differential equations. Here $u(x,t)$ is the unknown m-dimensional vector function, $f(u)$ is the flux vector, $g(u)$ is a continuous source vector function, with x the single spatial coordinate and t the temporal coordinate. For the numerical integration of (2.1) we consider uniform spatial and temporal grids with the spacings, $\Delta x{=}x_{j+1} - x_j$; $\Delta t{=}t^{n+1} - t^n$ (with j and n being suitable integer indices) and employ the non-staggered-grid version [3] of [2]:

$$\begin{aligned}
\bar{u}_j^{n+1} \;=\;& \frac{1}{4}\left(\bar{u}_{j+1}^n + 2\bar{u}_j^n + \bar{u}_{j-1}^n\right) - \frac{1}{16}\left(u_{xj+1}^n - u_{xj-1}^n\right) - \frac{1}{8}\left[u_{xj+\frac{1}{2}}^{n+1} - u_{xj-\frac{1}{2}}^{n+1}\right] \\
&+\frac{\Delta t}{8}\left[g\left(u_{j+1}^n\right) + 2g\left(u_j^n\right) + g\left(u_{j-1}^n\right)\right] \\
&+\frac{\Delta t}{8}\left[g\left(u_{j+1}^{n+1}\right) + 2g\left(u_j^{n+1}\right) + g\left(u_{j-1}^{n+1}\right)\right] \\
&-\frac{\lambda}{4}\left[\left(f_{j+1}^n - f_{j-1}^n\right) + \left(f_{j+1}^{n+1} - f_{j-1}^{n+1}\right)\right]\,,
\end{aligned} \tag{2.2}$$

where $\lambda = \Delta t/\Delta x$ and the subscript x denotes differentiation with respect to x. This scheme has been obtained by extending the scheme [2] based on a staggered spatial grid to one based on a non-staggered grid, following the procedure outlined in [4]. In addition, we have also incorporated a non-zero source term $g(u)$ so that (2.1) above can be applied to non-homogeneous systems. Full details are available from the authors [3]. Consequently, of course, it is much easier to apply boundary conditions on non-staggered grids. Further, in order to apply this scheme it is customary to employ suitable non-oscillatory derivative approximations. In all our calculations we used the "UNO" derivative approximation [2] for the derivative terms indicated by the subscript x in (2.1). In particular we utilize the form,

$$\begin{aligned}
u_{xj} \;=\;& MM(u_j - u_{j-1} + \frac{1}{2}MM(u_j - 2u_{j-1} + u_{j-2}, u_{j+1} - 2u_j + u_{j-1}), \\
& u_{j+1} - u_j - \frac{1}{2}MM(u_{j+1} - 2u_j + u_{j-1}, u_{j+2} - 2u_{j+1} + u_j))\,,
\end{aligned} \tag{2.3}$$

where the min-mod non-linear limiter MM is defined by

$$MM(s_1, s_2, ...) = \begin{cases} \min\{s_j\} \ if \ s_j > 0 \quad \forall j \\ \max\{s_j\} \ if \ s_j < 0 \quad \forall j \\ 0 \quad otherwise\,. \end{cases}$$

Many other derivative approximations are used in practice (see for example [5]).

3. **Boundary conditions**

3.1. **Absorption.** In this section we examine boundary conditions conditions for absorbing shocks.

First for computation over $x \in [x_L, x_R]$ with corresponding $j = L, L+1, ..., R-1, R$, we note from (2.2) and (2.3) that the spatial index range must be $L+2 \leq j \leq R-2$. Thus the u-values at the grid points corresponding to $j = L, L+1$ and $j = R-1, R$ need to be computed at the next time level. For complete absorption we employ successive double quadratic extensions in the forms:

$$u_{L+1} = u_{L+4} - 3u_{L+3} + 3u_{L+2}\,, \quad u_L = u_{L+3} - 3u_{L+2} + 3u_{L+1}\,, \tag{3.1}$$

$$u_{R-1} = u_{R-4} - 3u_{R-3} + 3u_{R-2}\,, \quad u_R = u_{R-3} - 3u_{R-2} + 3u_{R-1}\,, \tag{3.2}$$

which apply respectively to the left ($j = L, L+1$) and right ($j = R-1, R$) boundaries. These expressions can be shown to be second order accurate in the grid spacing Δx and hence are consistent with the second-order numerical scheme (2.2). Issues relating to the specific components on which they are to be applied are discussed in the next section.

3.2. **Reflection.** For reflection of a shock we shall find that specifically the density component should satisfy the homogeneous Neumann condition ($\partial u/\partial x = 0$), and quadratic extensions for the other two components again on two successive points at each end as above. We thus employ the successive Neumann conditions:

$$u_{L+1} = (4u_{L+2} - u_{L+3})/3;\ u_L = (4u_{L+1} - u_{L+2})/3 \tag{3.3}$$

$$u_{R-1} = (4u_{R-2} - u_{R-3})/3;\ u_R = (4u_{R-1} - u_{R-2})/3. \tag{3.4}$$

These are one-sided derivatives which can again be shown to be second-order accurate and thus consistent with (2.2). An interpretation of these conditions is given in the context of the applications below. In the following we present two test cases.

4. **Test applications**

4.1. **Burgers' equation.** First, as a simple illustration we apply the scheme (2.2) to the one-dimensional inviscid Burgers' equation:

$$\frac{\partial u(x,t)}{\partial t} + \frac{1}{2}\frac{\partial\left(u^2\right)}{\partial x} = 0,$$
$$u(x,0) = u_0(x), \quad t > 0. \tag{4.1}$$

A characteristic analysis [1] of this system admits waves that propagate with a constant speed in one direction only. Hence we can only expect to study absorption of a disturbance into a boundary and no reflection from it. Further, it is well known [1] that any initial waveform will evolve into a shock or a rarefaction wave. We allow for the smooth passage of such a shock by setting the outflow conditions (3.2). These naturally allow free adjustment of the flow, thus catering for smooth absorption. Figure 1 depicts a typical initial condition, which evolves into a shock. Frame (b) depicts the situation when the shock has moved close to the boundary and illustrates smooth oscillation-free absorption. Frame (c) depicts the situation when the shock has been fully absorbed, resulting in a newer equilibrium level.

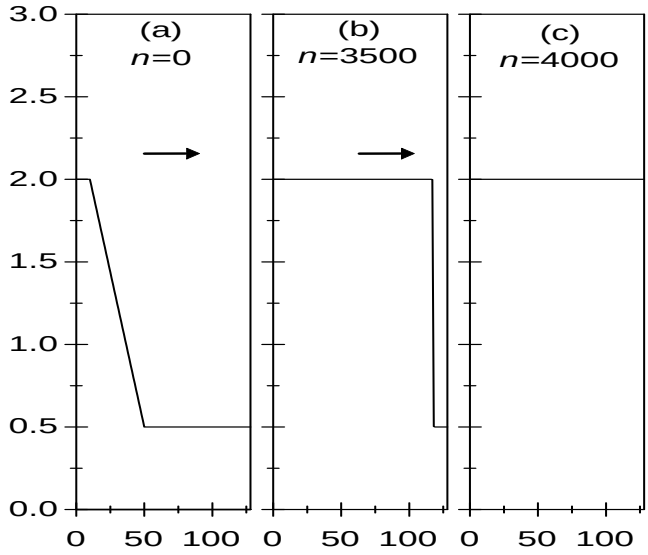

Figure 1. Absorption of a Burgers' equation shock. The plots show $u(x,t)$ as a function of the x-coordinate at fixed times $t = n \times 0.01$

4.2. **Broadwell gas model.** In this case we consider a multi-component problem modelled by the Broadwell gas equations [6,7],

$$\frac{\partial \rho}{\partial t} + \frac{\partial m}{\partial x} = 0, \quad \frac{\partial m}{\partial t} + \frac{\partial z}{\partial x} = 0, \quad \frac{\partial z}{\partial t} + \frac{\partial m}{\partial x} = \frac{1}{\varepsilon}\left(\rho^2 + m^2 - 2\rho z\right). \tag{4.2}$$

Here ε is the mean free path and $\rho(x,t), m(x,t), z(x,t)$ are the density, momentum and flux, respectively. For illustration we compute the 'stiff' case with $\varepsilon = 10^{-8}$ on a fine grid with $\Delta t = 0.1 \times \varepsilon$ and $\Delta x = 3 \times \Delta t$. An analysis [6,7] of the corresponding eigensystem shows that both left and right moving waves are admissible, with characteristic speeds of +1, -1, and 0. Thus we can propagate waves from the left and also obtain waves that can be reflected back into the system from the boundaries.

In order to achieve this for shocks, we choose a typical Riemann initial condition to produce a right propagating shock, such as,

$$\text{Rim1}: \begin{cases} \rho = 2, m = 1, z = 1; & x < 200 \\ \rho = 1, m = 0.13962, z = 1; & x > 200 \end{cases}$$

on $0 \leq x \leq 800$.

Then in the first instance we choose for the boundary conditions the free flow conditions (3.1)-(3.2) to study shock absorption. Figure 2 (a)-(b) depicts the situation of smooth absorption of the shock after about $t = 2300 \times \varepsilon \times 0.01$.

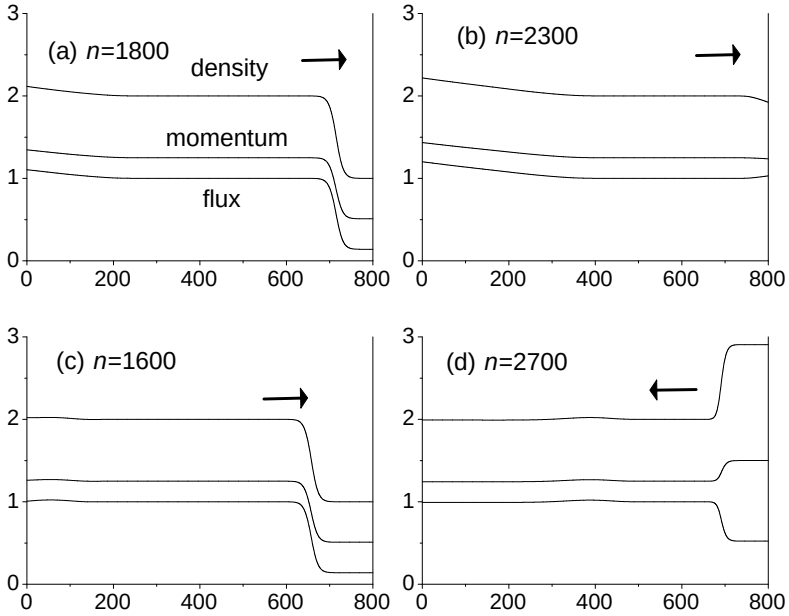

Figure 2. Absorption: (a)-(b) and reflection: (c)-(d) of Broadwell gas shocks at various time steps n. Plots of the density $\rho(x,t)$, momentum $m(x,t)$ and flux $z(x,t)$ are shown as functions of the x-coordinate

In the second instance to study shock reflection, we employ the same initial conditions but with the Neumann condition (3.4) on the density, together with the free flow conditions (3.2) on the momentum and flux. Here again, Figure 2 (c)-(d) shows that the shock is smoothly reflected with no spurious oscillations. The interpretation of the boundary conditions in this case may be seen as follows: the Neumann condition for the density forces the density profile at the boundary to level off, i.e. to prohibit any density gradient from forming. The latter would be the case when for example, free-flow density profiles are imposed. Thus since the momentum and flux fields are allowed to freely adjust for this condition, the fluid near the right boundary will be forced to dam-up due to the flow from the left, resulting in increasing density at the right. This continues until the upstream shock level has completely reached the boundary. Then the resulting compression in the vicinity of the right boundary

will tend to propagate out back into the system. This propagating front develops into a shock which travels to the left, with a higher upstream level. Use of such a homogeneous Neumann condition has also been made in other studies of shock reflection, for example in a two-dimensional shock tube problem [8]. We find such a device to be a good way to smoothly reflect the shock from the right boundary.
Whilst there are more sophisticated boundary conditions that have been reported in the literature [1,9,10,11], we are not aware of studies of their applicability to shock propagation. For example, in [9], apart from physical boundary conditions, soft or numerical ones are formulated which are treated as additional compatibility relations. These are obtained by considering the passage of inflowing and outflowing linear waves corresponding to the characteristics of the problem. Their wave amplitudes are then computed from the solution of additional local one-dimensional inviscid (LODI) relations which are compatible with the conservation laws and which have to be solved at the boundaries. Then for outgoing waves the internal grid values determine the boundary values, whilst for incoming (or reflected) waves and for other variables required by the numerical scheme the LODI relations are used. To obtain some correspondence between our simple approach for shock reflection and the corresponding LODI relations of Poinsot and Lele [9] we proceed as follows: we note that their LODI relations (which we extract for one-dimension $\sim x_1$ coordinate) and which they determined by examining the corresponding inviscid flow corresponding to ideal gas Navier-Stokes equations are

$$\begin{aligned}
\frac{\partial \rho}{\partial t} + \frac{1}{c^2}\left[A_2 + \frac{1}{2}(A_5 + A_1)\right] &= 0, \\
\frac{\partial p}{\partial t} + \frac{1}{2}\left(A_5 + A_1\right) &= 0, \\
\frac{\partial u_1}{\partial t} + \frac{1}{2\rho c}\left(A_5 - A_1\right) &= 0, \\
A_1 = (u_1 - c)\left(\frac{\partial p}{\partial x_1} - \rho c \frac{\partial u_1}{\partial x_1}\right), & \\
A_5 = (u_1 + c)\left(\frac{\partial p}{\partial x_1} + \rho c \frac{\partial u_1}{\partial x_1}\right), &
\end{aligned}$$

where $p, \rho, u_1, c, A_1, A_5$ are the pressure, density, flow velocity, speed of sound, incoming (or reflected) wave amplitude and outgoing wave amplitude, respectively.

Now, for reflection at a solid boundary one can set the physical condition $u_1 = 0$ for all times. Then with

$$\frac{\partial u_1}{\partial t} = \frac{\partial u_1}{\partial x_1} = 0 \tag{4.3}$$

at the boundary, the above implies that

$$\frac{\partial p}{\partial x_1} = 0 \tag{4.4}$$

there. We observe that this condition on the density coincides with our choice (homogeneous Neumann) employed in the Broadwell gas case above.

Finally, we should mention that their particular LODI relations quoted here are valid for the case of an ideal gas, and, to our understanding, for smooth wave propagation and thus one cannot infer its validity for shock propagation. In [10] however, their approach is extended for more realistic gases, but still without consideration of shock propagation. Another point to make here is that the type of numerical scheme employed also determines the extent or number of these further boundary or compatibility relations. These are nevertheless interesting questions which are matters for further investigation. In contrast here, we are formulating and testing simple local conditions which are computationally inexpensive.

5. **Conclusion**

We have outlined and tested some simple boundary conditions that can be used with a class of high resolution central difference schemes which are commonly employed in studies of shock capturing and wave propagation. In particular, when we employ these boundary conditions successively on a boundary point and its immediate neighbour, a device which we designate as "thick" boundary conditions, our tests indicate that smooth shock absorption and reflection can occur. These simple local boundary conditions are thus expected to be useful for other similar difference schemes.

REFERENCES

1. Godlewski, E. and Raviart, P.-A.: *Numerical Approximation of Hyperbolic Systems of Conservation Laws*, Springer-Verlag, New York, 1996.
2. Nessyahu, H. and Tadmor, E.: *Non-oscillatory central differencing for hyperbolic conservation laws*, Journal of Computational Physics, **87**, (1990), 408-463.
3. Naidoo, R. and Baboolal, S.: *Numerical Integration of the Plasma Fluid Equations with a Non-Staggered Modification of the Second-Order Nessyahu-Tadmor Central Scheme and Soliton Modelling*, University of Durban-Westville Computer Science Research Report CSCR-2003/01, (2003), 1-14.
4. Jiang, G.-S., Levy, D., Lin, C.-T., Osher, S. and Tadmor, E.: *High-resolution non-oscillatory central schemes with non-staggered grids for hyperbolic conservation laws*, SIAM Journal on Numerical Analysis, **35**, (1998), 2147-2168.
5. Kurganov, A. and Tadmor, E.: *New high-resolution central schemes for nonlinear conservation laws and convection-diffusion equations*, Journal of Computational Physics, **160**, (2000), 241-282.
6. Caflisch, R.E., Jin, Shi and Russo, G.: *Uniformly accurate schemes for hyperbolic systems with relaxation*, SIAM Journal on Numerical Analysis, **34**, (1997), 246-281.
7. Jin, Shi: *Runge-Kutta methods for hyperbolic conservation laws with stiff relaxation terms*, Journal of Computational Physics, **122**, (1995), 51-67.
8. Banda, M.K. and Seaid, M.: *A Class of the Relaxation Schemes for the Two-Dimensional Euler Systems of Gas Dynamics*, Lecture Notes in Computer Science, Springer-Verlag, 2329, (2002), 930-939.
9. Poinsot, T. J. and Lele, S. K.: Boundary conditions for direct simulations of compressible viscous flows, *J. Comput. Phys.*, **101**, (1992), 104-129.

10. Baum, M., Poinsot, T. and Thevenin, D.: *Accurate boundary conditions for multicomponent reactive flows*, Journal of Computational Physics, **116**, (1994), 247-261.

11. Givoli, D.: *High-order nonreflecting boundary conditions without high order derivatives*, Journal of Computational Physics, **170**, (2001), 849-870.